Pergamon

Int. J. Solids Structures Vol. 35, No. 11, pp. 995–1008, 1998

0020–7683/98 $19.00 + .00

PII: S0020–7683(97)00103–0

STATISTICAL STRENGTH OF BRITTLE MATERIALS WITH STRONGLY INTERACTED COLLINEAR MICROCRACKS

SU-LIN ZHANG, TENG LI and WEI YANG*
Department of Engineering Mechanics, Tsinghua University, Beijing 100084, Peoples' Republic of China
E-mail: yw-dem@mail.tsinghua.edu.cn

(*Received* 16 *July* 1996; *in revised form* 17 *March* 1997)

Abstract—The coalescing process from microcracks to a fatal macroscopic crack is dominated by the strong interaction among neighbouring microcracks. The distribution of microcracks modifies the strength and toughness of a brittle material. The present paper focuses on the case of strongly interacting collinear microcracks, and quantifies the influence by the statistical distributions of crack lengths and ligament sizes. The strength of a brittle solid decreases as the standard deviation of those distributions increases. Furthermore, we predict the scale dependency of brittle materials: a specimen of large size would have lower strength than a small specimen with the same microcrack density. The analysis indicates that the statistical strength of a brittle material with strongly interacting collinear microcracks can be correlated by a three-parameter Weibull distribution. © 1998 Elsevier Science Ltd.

1. INTRODUCTION

Brittle materials are featured by the existence of randomly distributed microcracks. For a solid weakened by microcracks, considerable progresses have been achieved in estimating its overall stiffness. The overall stiffness can be accurately estimated through the self-consistent method (Budiansky and O'Connell, 1976), the generalized self-consistent method (Christensen and Lo, 1979), and Mori–Tanaka method (Mori and Tanaka, 1973; Taya and Chou, 1981). The above-mentioned homogenization methods, however, are suspectable for the strength estimate of brittle materials.

Experiments (Evans and Wiederhorn, 1984; Wiederhorn and Fuller, 1985) revealed that the strength and toughness of brittle materials are sensitive to the microstructures and exhibit a wide Weibull distribution. For a brittle material of fixed crack density and average crack length, the statistical distribution of the strength declines as the specimen size increases, or as the deviation of crack lengths (or ligament lengths) increases.

The scattering in the strength of brittle materials suggests a statistical theory. Weibull (1939) introduced a principle which states that a material breaks when the weakest microcrack in the material leads to a fatal crack. The above weakest link theory (WLT) formed the basis of many subsequent statistical models for the failure prediction of brittle materials. Batdorf and Crose (1974) extended the analysis of Weibull to the cases of multiaxial stress state. A parallel analysis was also conducted by Rufin *et al.* (1984) by incorporating WLT with the independent action theory. Evans (1978) developed a statistical analysis for distributed penny-shaped cracks based on a critical strain-energy fracture criterion. Recently, She *et al.* (1991) derived a formula for evaluating the failure probabilities of brittle materials under a general fracture criterion, which contains the models mentioned above as the special cases. Experimental results were presented (She and Landes, 1993) to support their analysis.

These models can explain the strength data of brittle materials to some extent, but nevertheless share a common weakness: the strong interaction among nearby microcracks, as well as its role in the coalescing process to form a fatal crack, has not been addressed.

* Author to whom correspondence should be addressed.

In the present work, we formulate the coalescing process of microcracks strictly as the outcome of interacting stress intensity factors (SIF). The interacting SIF for collinear microcracks can be estimated by a method proposed by Kachanov (1985, 1987). The accuracy of this evaluation is verified by checking its prediction against the numerical solution of the original system of integral equations. Based on this estimate of strongly interacted microcracks, we propose a statistical analysis to predict the failure probabilities of an infinite plate containing collinear microcracks. Two simple cases are examined in detail. The first case concerns N collinear microcracks of equal length, but with distributed ligament sizes. The second case concerns N collinear microcracks of distributed lengths separated by ligaments of equal size. Theoretical analysis and examples for each case are presented. Examples for both cases are verified by direct numerical simulations on statistically generated collinear microcrack configurations. The statistical predictions for the two cases are correlated by Weibull analyses, a relationship between the Weibull modulus and the standard deviation of the ligament size (or crack length) is established.

2. STRESS INTENSITY FACTORS OF COLLINEAR MICROCRACKS

We first discuss the problem of N collinear microcracks with arbitrary lengths and ligament sizes in an otherwise infinite plate loaded by uniform remote tension σ^∞. An integral representation of such problem was discussed by Rice (1968). An alternative way to solve the problem is through superposition technique, which can be generalized to the case of oriented microcrack distributions in a plane [see Gong and Horii (1989)]. To solve the stress intensity factors, one replaces the original problem by an equivalent configuration: the plate is stress free at infinity, but with uniform traction σ^∞ applied along the faces of every microcracks. The latter problem is further reduced to the superposition of N problems, each involves an infinite plate with a single crack at the designated location. The crack faces are loaded by normal traction yet to be solved. For the problem concerning with the ith microcrack, the hypothetical traction $\sigma_i(x)$ along the crack faces is the sum of σ^∞ and the normal stresses induced by the (unknown) traction applied on the faces of other microcracks. For collinear microcracks, one has

$$\sigma_i(x) = \sigma^\infty + \frac{1}{\pi}\sum_{j=1,j\neq i}^{N}\frac{1}{\sqrt{(x-b_j)^2-a_j^2}}\int_{b_j-a_j}^{b_j+a_j}\frac{\sqrt{a_j^2-\xi^2}}{|x-b_j-\xi|}\sigma_j(\xi)\mathrm{d}\xi,\ i=1,2,\ldots N \tag{1}$$

where a_j and b_j denote the half-length and the center location of the jth microcrack. Accurate solution for the above system of integral equations can be obtained through the Chebyshev polynomial technique. The stress intensity factors of the ith microcrack are:

$$K_i^{\text{left}} = \frac{1}{\sqrt{\pi a_i}}\int_{-a_i}^{a_i}\sqrt{\frac{a_i-x}{a_i+x}}\sigma_i(x)\mathrm{d}x,\quad K_i^{\text{right}} = \frac{1}{\sqrt{\pi a_i}}\int_{-a_i}^{a_i}\sqrt{\frac{a_i+x}{a_i-x}}\sigma_i(x)\mathrm{d}x \tag{2}$$

where the superscript "left" (or "right") refers to the left (or the right) crack tip.

To simplify the solution, Kachanov (1985, 1987) replaced the non-uniform tractions in the integrand of eqn (1) by their average values. After solving N average tractions from N linear self-consistent equations, one is able to evaluate the non-uniform tractions from eqn (1), by replacing $\sigma_i(\xi)$ in the integrand of eqn (1) by its average $\langle\sigma_i(\xi)\rangle$. The stress intensity factors can be evaluated by Chebyshev polynomials as

$$K_i^{\text{right}} = \sigma^\infty\sqrt{\pi a_i} + \frac{\sqrt{\pi a_i}}{L}\sum_{j=1,j\neq i}^{N}\langle\sigma_j(x)\rangle\sum_{l=1}^{L}(x_l+1)\left[\frac{\left|x_l+\dfrac{b_i-b_j}{a_i}\right|}{\sqrt{\left(x_l+\dfrac{b_i-b_j}{a_i}\right)^2-\left(\dfrac{a_j}{a_i}\right)^2}}-1\right] \tag{3}$$

Table 1. Interacting SIF for two collinear cracks of equal length

c	Exact solution (Tada *et al.*)	SIF predicted by eqn (6)	Error (%)	SIF predicted by eqn (1)	Error (%)
0.4	1.112	1.112	0.0	1.112	0.0
0.2	1.255	1.251	0.3	1.255	0.0
0.1	1.473	1.452	1.4	1.473	0.0
0.04	1.905	1.809	5.0	1.924	1.0
0.02	2.372	2.134	10.0	2.419	2.0

where L denotes the number of integral points, and the locations $x_l = \cos[(2l-1)\pi/2L]$ $(l = 1, \ldots, L)$ are zeroes of Chebyshev polynomial. Without loss of generality, all derivations to follow are exemplified for the right crack tip, and the superscript "right" is omitted for brevity. The accuracy of this evaluation is verified by checking its prediction against the numerical solution of the integral equation system (1). Consider the special case of two collinear cracks along the x-axis, with crack tips taking the coordinates $(-1, -c/2)$ and $(c/2, 1)$. As shown in Table 1, the prediction by the estimate eqn (3) checks well with the exact solution [see Tada *et al.* (1973)], though the accuracy can be improved by directly solving the integral equation system (1).

3. STATISTICAL ANALYSIS

This section presents statistical analyses for the problem of N collinear microcracks in an infinite plate under uniform remote tension σ^∞. The half length of the microcrack is denoted by a, and the ligament size between two neighboring microcracks is denoted by c. Both a and c are statistical variables, and their statistical distributions are described by density functions $f(a)$ and $p(c)$, respectively. Both $f(a)$ and $p(c)$ are normalized, with c_-, a_-, c_+, a_+ being the lower and upper limits of c and a. Since the lengths of the microcracks and the ligament sizes between every two neighboring microcracks are statistical variables [see Fig. 1(a)], the solution of the stress intensity factors is burdensome. To simplify the problem, attention is focused on the strong interaction between the two neighboring microcracks (denoted by a' and a''), while the others are approximated by a periodically distributed crack array (with expected crack length $2a_0$ and ligament size c_0), as depicted in Fig. 1(b). By using the method of the previous section, the SIF at point A [see Fig. 1(b)] is

$$K_A = \sigma^\infty \sqrt{\pi a_0}\, F\left(\frac{c}{a_0}, \frac{a'}{a_0}, \frac{a''}{a_0}, \frac{c_0}{a_0}\right). \tag{4}$$

In eqn (4), F is a dimensionless shape function. Representative curves of the normalized stress intensity factor $(K_A/\sigma^\infty \sqrt{\pi a_0})$ at point A are plotted in Fig. 2. Figure 2(a) plots the $K_A/\sigma^\infty \sqrt{\pi a_0}$ vs c/a_0 curves under prescribed c_0/a_0 ratios, for the special case of $a' = a'' = a_0$. The normalized stress intensity factor increases as either the ligament size c or the average ligament size c_0 decreases. Figure 2(b) plots the $K_A/\sigma^\infty \sqrt{\pi a_0}$ vs a' a_0 curves under prescribed c_0/a_0 ratios, where $a'' = a_0$ and $c = c_0$. The normalized stress intensity factor increases as the average ligament size c_0/a_0 decreases or as the right crack length a'/a_0 increases. When $a' = a_0$ and $c = c_0$, the curves in Fig. 2(b) also describe the relation between $K_A/\sigma^\infty \sqrt{\pi a_0}$ and a''/a_0 under the same c_0/a_0 ratios. The number of microcracks, N, is taken as 100 in all calculations concerning Fig. 2.

In the two subsections to follow, we discuss two special cases: (A) collinear microcracks of equal length, but with ligaments of distributed sizes; and (B) collinear microcracks of the same ligaments, but distributed crack lengths. Both cases involve SIF estimates for N microcracks as described above.

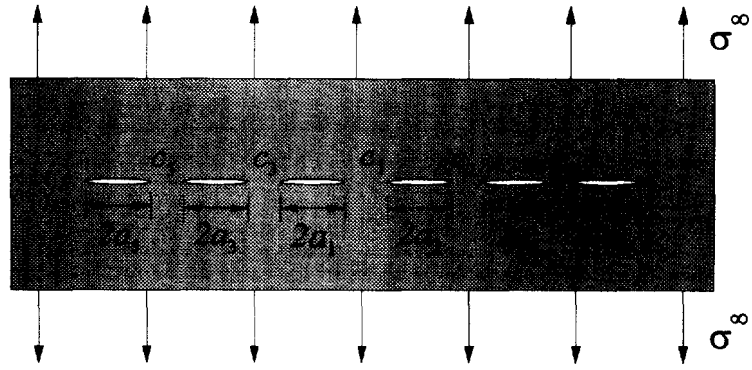

(a)

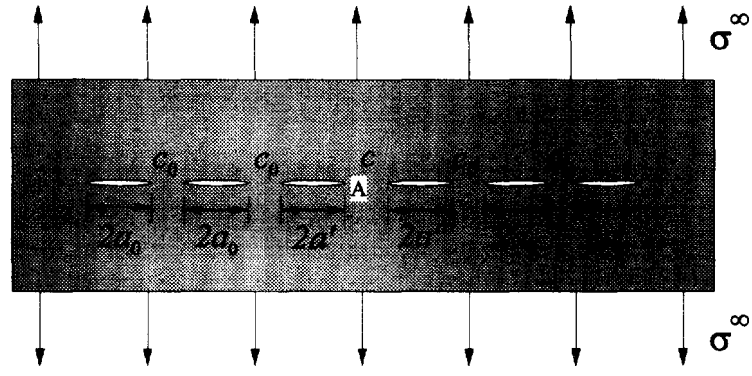

(b)

Fig. 1. Configurations of collinear microcracks: (a) array of microcracks with arbitrary lengths and ligament sizes; (b) array of microcracks with remote periodical configuration.

3.1. *Case A: equal length microcracks with ligaments of distributed sizes*

We first consider the case of microcracks of equal length, then the distribution $f(a)$ is a Dirac delta function $\delta(a-a_0)$ and $a' = a'' = a_0$. The distribution function for the ligament size $p(c)$ is a normalized distribution with c in the range of (c_-, c_+), where c_- and c_+ are the sizes of the minimum and the maximum ligaments. If the distribution $p(c)$ is very wide, c_- can be taken as zero. The average ligament size is given by $c_0 = \bar{c} = \int_{c_-}^{c_+} cp(c)\mathrm{d}c$. Note that K_A is a monotonically decreasing function of c/a_0, when $a' = a'' = a_0$ are fixed [Fig. 2(a)]. A threshold value of σ^∞, denoted by σ_{th}^∞, can be defined as

$$\sigma_{th}^\infty = \frac{K_{IC}}{\sqrt{\pi a_0}} \Big/ F\left(\frac{c_-}{a_0}, 1, 1, \frac{c_0}{a_0}\right) \tag{5}$$

where K_{IC} is the matrix fracture toughness. Corresponding to a given σ^∞ ($\sigma^\infty > 0$), one has a critical ligament size, denoted by c_{cr}^1, which satisfies the following equation

$$F\left(\frac{c_{cr}^1}{a_0}, 1, 1, \frac{c_0}{a_0}\right) = \frac{K_{IC}}{\sigma^\infty \sqrt{\pi a_0}}. \tag{6}$$

Equations (5) and (6) indicate that fracture cannot occur if $\sigma^\infty < \sigma_{th}^\infty$, and the whole

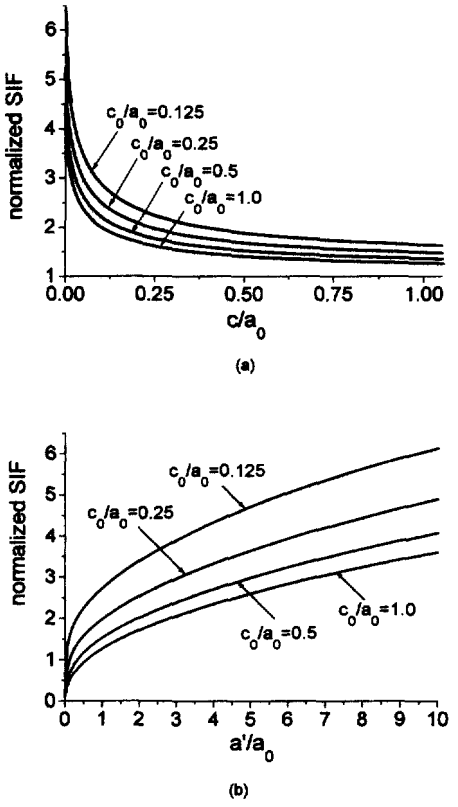

Fig. 2. Representative curves of the normalized stress intensity factor, $N = 100$: (a) $a' = a'' = a_0$; (b) $a' = a_0$, $c = c_0$.

structure remains intact. If $\sigma^\infty > \sigma_{th}^\infty$, the ligament of sizes smaller than c_{cr}^1 would break. The connection of the microcracks modifies the density functions $p(c)$ and $f(a)$ to

$$p_1(c) = \frac{p(c)}{1-\alpha} H(c - c_{cr}^1) \tag{7}$$

$$f_1(a) = \frac{1-2\alpha}{1-\alpha}\delta(a-a_0) + \frac{p(2a-4a_0)}{1-\alpha}[H(2a-4a_0-c_-) - H(2a-4a_0-c_{cr}^1)]. \tag{8}$$

In the above expressions, $\alpha = \int_{c_-}^{c_{cr}^1} p(c)\mathrm{d}c$ denotes the fraction of broken ligaments and H denotes the Heaviside step function. The first part of $f_1(a)$ denotes those unchanged microcracks of length $2a_0$, while the second part denotes the distribution density of microcracks formed by the ligament breaks. The expectations of the microcrack lengths and the ligament sizes after the first step of microcrack extension are denoted by

$$2\bar{a}_1 = 2\int_{a_0}^{2a_0 + 1/2c_{cr}^1} a f_1(a)\mathrm{d}a \quad \bar{c}_1 = \int_{c_{cr}^1}^{c_+} c p_1(c)\mathrm{d}c. \tag{9}$$

The failure of brittle solids is likely to be caused by the further connections between the extended microcracks and the microcracks of length $2a_0$. An extended microcrack has a length of $2a_1 = 4a_0 + c_1$, where c_1 falls within the range between c_- (the minimum ligament size) and c_{cr}^1 (the maximum ligament size which breaks under σ^∞). The failure process of a microcracked solid is determined by many event chains. Each chain consists of microcracks whose lengths are between $4a_0 + c_1$ and $4a_0 + c_1 + \mathrm{d}c_1$, with different c_1 values assigned to different chains. The solid will break if any chain breaks. Each chain is composed of $Np(c_1)\mathrm{d}c_1$ extended microcracks, and each of them is regarded as a link in the chain. The

chain will break if any link breaks. The failure of one extended microcrack proceeds by successive connections with the other microcracks. Each step in this coalescence sequence occurs with some possibility. As the connected crack grows longer, the possibility for further connection becomes larger. When the length of the extended crack reaches a critical size, the possibility for subsequent connection will reach unity. Each connection step is assumed as an isolated event, and scarcely modifies the overall ligament distribution $p_1(c)$. By utilizing eqn (4), the SIF at the right tip of this extended microcrack is

$$K^{\text{right}} = \sigma^{\infty}\sqrt{\pi\bar{a}_1}\,F\left(\frac{c}{\bar{a}_1}, \frac{a_1}{\bar{a}_1}, 1, \frac{\bar{c}_1}{\bar{a}_1}\right). \tag{10}$$

If $K^{\text{right}} \geqslant K_{\text{IC}}$, the crack extends and connects to a nearby microcrack of expected length $2\bar{a}_1$. Corresponding to the value of $2a_1$, one can find a critical length of c, denoted by c_{cr}^2, which satisfies the following equation

$$K_{\text{IC}} = \sigma^{\infty}\sqrt{\pi\bar{a}}\,F\left(\frac{c_{\text{cr}}^2}{\bar{a}_1}, \frac{a_1}{\bar{a}_1}, 1, \frac{\bar{c}_1}{\bar{a}_1}\right). \tag{11}$$

Equation (11) suggests that the microcrack of length $2a_1$ will connect to the nearby microcrack of length $2\bar{a}_1$ if the ligament size c between them falls in the range of $(c_{\text{cr}}^1, c_{\text{cr}}^2)$. Consequently, the probability for the extension of the microcrack of length $2a_1$ is $\int_{c_{\text{cr}}^1}^{c_{\text{cr}}^2} p_1(c)\mathrm{d}c$. When the steps above are repeated, the crack length becomes

$$2a_n = 4a_0 + 2(n-1)\bar{a}_1 + c_1 + \sum_{k=2}^{n} \bar{c}_k(c_1) \tag{12}$$

after n successive connections. The expectation for the ligament size during the kth connection is

$$\bar{c}_k = \frac{\displaystyle\int_{c_{\text{cr}}^1}^{c_{\text{cr}}^k} c p_1(c)\mathrm{d}c}{\displaystyle\int_{c_{\text{cr}}^1}^{c_{\text{cr}}^k} p_1(c)\mathrm{d}c} \qquad k = 2,3,\ldots \tag{13}$$

where symbol c_{cr}^k denotes the critical size of ligaments for the kth connection, given by

$$K_{\text{IC}} = \sigma^{\infty}\sqrt{\pi\bar{a}_1}\,F\left(\frac{c_{\text{cr}}^k}{\bar{a}_1}, \frac{a_{k-1}}{\bar{a}_1}, 1, \frac{\bar{c}_1}{\bar{a}_1}\right) \quad k = 2,3,\ldots. \tag{14}$$

Please note that the $\bar{c}_k$, $k = 2,3,\ldots$. in eqn (13) bears different physical meaning from the $\bar{c}_1$ in eqn (9). The total number of microcrack connections, M, before the emergence of a fatal crack, is determined by

$$a_{M-1} < \frac{1}{\pi}(K_{\text{IC}}/\sigma^{\infty})^2 \leqslant a_M. \tag{15}$$

For the microcrack of length $2a_1$, its failure probability is unity if $M = 1$. Otherwise, it is equal to the product of the successive connecting possibilities

$$P_f(c_1) = \prod_{n=2}^{M} \int_{c_{cr}^1}^{c_{cr}^n} p_1(c)\mathrm{d}c. \tag{16}$$

Then its survival probability is

$$P_s(c_1) = 1 - P_f(c_1). \tag{17}$$

There are $Np(c_1)\mathrm{d}c_1$ microcracks of almost identical length $2a_1$. According to WLT, each microcrack consists of a link in the chain. Assume the breaking process of a link is independent of the others, then the survival probability of the chain is equal to the multiplications of the survival probabilities of $Np(c_1)\mathrm{d}c_1$ links. Thus we have

$$P_s = \{1 - P_f(c_1)\}^{Np(c_1)\mathrm{d}c_1} \approx \exp\{-NP_f(c_1)p(c_1)\mathrm{d}c_1\}. \tag{18}$$

The approximation in the last step comes from the fact that the increment $NP_f(c_1)p(c_1)\mathrm{d}c_1$ is much smaller than unity. Again from WLT, the cumulative survival probability is the product of the survival probabilities of all connected microcracks. Thus, one has

$$P_{surv} = \exp\left\{-N \int_{c_-}^{c_{cr}^1} P_f(c)p(c)\mathrm{d}c\right\}. \tag{19}$$

Finally, the failure probability for the brittle solid containing N microcracks is

$$P_{fail} = 1 - \exp\left\{-N \int_{c_-}^{c_{cr}^1} P_f(c)p(c)\mathrm{d}c\right\} \tag{20}$$

provided that $\sigma^\infty \geqslant \sigma_{th}^\infty$.

From eqn (20), the failure probability P_{fail} depends on the number of microcracks, the distribution of the ligaments, the average crack density, and the level of the applied stress. The influence of σ^∞ can be observed from its relations to c_{cr}^1 and P_f. For the special case of a periodic crack array, the failure probability is reduced to $P_{fail} = H(\delta^\infty - \sigma_{th}^\infty)$.

Figure 3 plots the failure probability versus the normalized strength $\sigma^\infty\sqrt{\pi a_0}/K_{IC}$ curve. We prescribe $p(c)$ by a normal distribution which peaks at $c = c_0$. The dimensionless standard deviation s is normalized with respect to c_0. The calculations are conducted under a crack density of $c_0/a_0 = 0.25$. Figure 3(a) is plotted under a fixed standard deviation of s, with different curves corresponding to the N values of 100, 200, 500 and 1000. The failure probability slowly rises when σ^∞ exceeds the threshold value σ_{th}^∞, then undergoes a transition stage, and finally approaches the asymptote of $P_{fail} = 1$. The graph depicts that the transition strength level for a brittle solid decreases as the number of microcracks increases, which predicts the scaling effect (or the specimen size dependence) of brittle solids. In Fig. 3(b), the number of microcracks is fixed at 300, with different curves corresponding to the s values of 0, 0.1, 0.15, 0.2, 0.25 and 0.3. Under the same crack density, a brittle solid with non-uniform ligament sizes would have a strength considerably lower than the one with relatively uniform ligament sizes.

3.2. *Case B: collinear microcracks of distributed lengths*

We next discuss N microcracks separated by ligaments of fixed size c_0, while $f(a)$ is a normalized distribution function with average crack length $2a_0$. The value of a ranges from the maximum possible half crack length a_- to the minimum possible half crack length a_+. Without loss of generality, we consider the interaction between two neighboring cracks of lengths $2a_L$ (long microcrack) and $2a_S$ (short microcrack), with $a_L > a_S$. The interacted SIF at the tip of long microcrack is

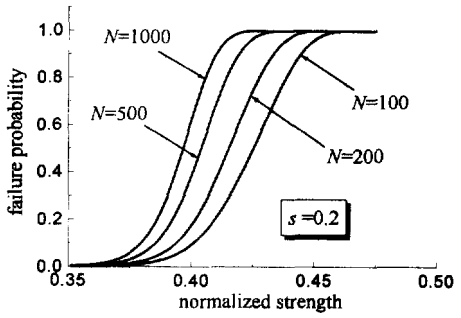

(a)

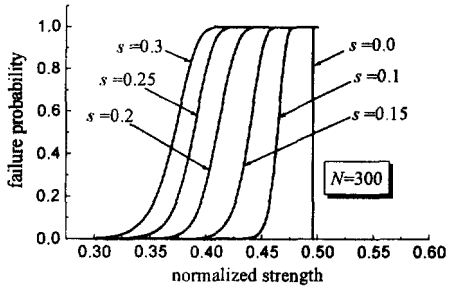

(b)

Fig. 3. Failure probability vs normalized strength of brittle solids, case A : (a) $s = 0.2$; (b) $N = 300$.

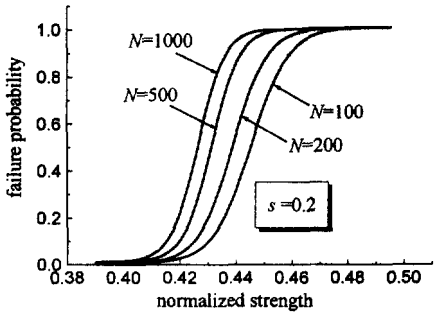

(a)

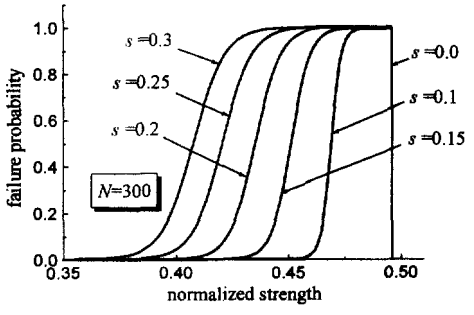

(b)

Fig. 4. Failure probability vs normalized strength of brittle solids, case B : (a) $s = 0.2$; (b) $N = 300$.

$$K = \sigma^{\infty}\sqrt{\pi a_0}\, F\left(\frac{c_0}{a_0}, \frac{a_L}{a_0}, \frac{a_S}{a_0}, \frac{c_0}{a_0}\right). \tag{21}$$

Figure 2(b) shows that K is a monotonically increasing function of both a_L/a_0 and a_S/a_0. The threshold value of σ^{∞}, σ^{∞}_{th}, refers to the special case of $a_L = a_S = a_+$

$$\sigma^{\infty}_{th} = \frac{K_{IC}}{\sqrt{\pi a_0}} \Big/ F\left(\frac{c_0}{a_0}, \frac{a_+}{a_0}, \frac{a_+}{a_0}, \frac{c_0}{a_0}\right). \tag{22}$$

If $\sigma^{\infty} < \sigma^{\infty}_{th}$, no ligaments break. Otherwise, a number of ligaments will break, and there exists an $a^* \leqslant a_+$, such that

$$F\left(\frac{c_0}{a_0}, \frac{a^*}{a_0}, \frac{a^*}{a_0}, \frac{c_0}{a_0}\right) = \frac{K_{IC}}{\sigma^{\infty}\sqrt{\pi a_0}}. \tag{23}$$

A long microcrack with half length $a_L \leqslant a^*$ cannot connect to any microcracks shorter than itself. On the other hand, if $a_L > a^*$, one can find a critical value of a_S, denoted by a^1_{cr}, which meets the following equation

$$F\left(\frac{c_0}{a_0}, \frac{a_L}{a_0}, \frac{a^1_{cr}}{a_0}, \frac{c_0}{a_0}\right) = \frac{K_{IC}}{\sigma^{\infty}\sqrt{\pi a_0}}. \tag{24}$$

The long microcrack a_L can connect with any short microcracks whose lengths exceed than $2a^1_{cr}$. Therefore, the total connecting probability of ligaments is

$$\beta = \int_{a^*}^{a_+} f(a_L) \int_{a^1_{cr}}^{a_L} f(a)\mathrm{d}a\mathrm{d}a_L. \tag{25}$$

After the first connection, the long microcracks of length $2a_L$ change to the ones of length $2a_1 = 2a_L + c_0 + 2a_S$, with a_S taking distributed values. Moreover, the same number of short microcracks disappear, and the total number of the microcracks becomes $N(1-\beta)$. The probability density function of the microcrack lengths changes to

$$f_1(a) = \frac{f(a)}{1-\beta}\left[1 - H(a-a^*)\int_{a^1_{cr}(a)}^{a} f(a)\mathrm{d}a - \int_{\max(a^*,a)}^{a_+} H(a-a^1_{cr}(a_L))f(a_L)\mathrm{d}a_L\right]$$
$$+ \frac{1}{1-\beta}\int_{a^*}^{a_+} f(a_L) f\left(a - a_L - \frac{c_0}{2}\right) H\left(2a_L - a + \frac{c_0}{2}\right) H\left(a - a_L - \frac{c_0}{2} - a^1_{cr}(a_L)\right)\mathrm{d}a_L. \tag{26}$$

In the right-hand side of eqn (26), the first line denotes the distribution density of unchanged microcracks, whereas the second line denotes the distribution density of extended microcracks. It is those extended microcracks that are most likely to create a fatal crack.

Similar to the discussion in case A, we take a connected microcrack of length $2a_1$ as a link of a chain of the whole structure, and follow the process of its successive connections. After the first step of microcrack connections, the expected length of microcracks is

$$2\bar{a}_1 = 2\int_{a_-}^{2a_+ + 1/2c_0} a f_1(a)\mathrm{d}a. \tag{27}$$

Corresponding to the value $2a_1$, we can find the next critical value of a_S, denoted by a^2_{cr}, which satisfies the following equation

$$F\left(\frac{c_0}{\bar{a}_1}, \frac{a_1}{\bar{a}_1}, \frac{a_{cr}^2}{\bar{a}_1}, \frac{c_0}{\bar{a}_1}\right) = \frac{K_{IC}}{\sigma^\infty \sqrt{\pi \bar{a}_1}}. \tag{28}$$

Equation (28) suggests that the extended microcrack of length $2a_1$ will connect to a nearby microcrack a_S if a_S is longer than a_{cr}^2.

When the steps in case A are repeated, the crack length after n successive connections, $2a_n$, is given by

$$2a_n = 2a_1 + (n-1)c_0 + 2\sum_{k=2}^{n} \bar{a}_k \tag{29}$$

where

$$\bar{a}_k = \int_{a_{cr}^k}^{a_+} a f_1(a)\mathrm{d}a \Big/ \int_{a_{cr}^k}^{a_+} f_1(a)\mathrm{d}a \quad k = 2,3,\ldots \tag{30}$$

is the expected length of the microcrack that connects to the extending crack during the kth connection. In eqn (30), $2a_{cr}^k$ denotes the critical crack length for the kth connection, defined by

$$f\left(\frac{c_0}{\bar{a}_1}, \frac{a_{k-1}}{\bar{a}_1}, \frac{a_{cr}^k}{\bar{a}_1}, \frac{c_0}{\bar{a}_1}\right) = \frac{K_{IC}}{\sigma^\infty \sqrt{\pi \bar{a}_1}}. \tag{31}$$

Please note that the $\bar{a}_k$, $k = 2,3,\ldots,$ in eqn (30) bears different physical meaning from the $\bar{a}_1$ in eqn (27). The total number of stable microcrack connections, M, before the emergence of a fatal crack, is still determined by eqn (15). The failure probability of one microcrack with a first connection length of $2a_1$ can be calculated by the following multiplicative formula which accounts for the successive connections

$$P_f(a_1) = \prod_{n=1}^{M} \int_{a_{cr}^n}^{a_+} f_1(a)\mathrm{d}a. \tag{32}$$

If the same procedure in the previous subsection is followed, the failure probability for the brittle solid containing N microcracks is

$$P_{fail} = 1 - \exp\left\{-N(1-\beta)\int_{a_+}^{2a_+ + 1/2c_0} P_f(a) f_1(a)\mathrm{d}a\right\} \tag{33}$$

provided that $\sigma^\infty \geqslant \sigma_{th}^\infty$.

Figure 4 plots the failure probabilities vs the normalized strength $\sigma^\infty \sqrt{\pi a_0}/K_{IC}$. We prescribe $f(a)$ by a normal distribution which peaks at $c_0 = 0.25a_0$. The dimensionless standard deviation s is normalized with respect to a_0. Figure 4(a) is plotted under a fixed standard deviation of $s = 0.2$, with different curves corresponding to the N values of 100, 200, 500 and 1000. Figure 4(b) fixes the number of microcracks at 300, with different curves corresponding to the s values of 0, 0.1, 0.15, 0.2, 0.25 and 0.3. Trends similar to those in Fig. 3 are predicted for collinear microcracks of distributed lengths.

4. DIRECT NUMERICAL SIMULATIONS

Configurations of scattered collinear microcracks are generated according to prescribed s and N values. The number of different configurations generated under the same s and N values is termed the random generation number, N_g. Those microcrack configurations are analyzed numerically by solving the integral equation (1). When the maximum stress

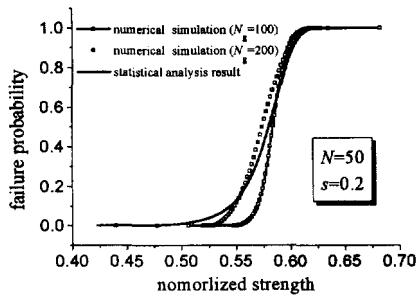

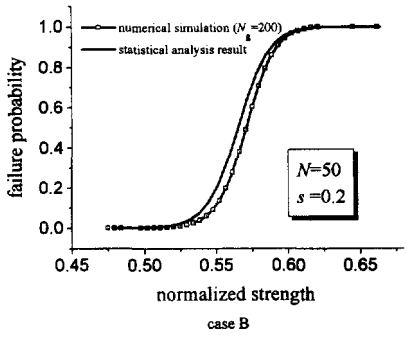

Fig. 5. Comparisons between the statistical predictions and direct numerical simulations of material strengths, $s = 0.2$, $N = 50$: case A; (b) case B.

intensity factor K_{max} (among all crack tips) reaches K_{IC}, we connect that crack tip to the nearby microcrack. The modified configuration is analyzed again to obtain the remote stress level for the next microcrack connection. That coalescence process can be simulated step by step, until a critical remote stress for catastrophic fracture is reached. That critical stress is termed the strength σ^{∞} of the brittle solid containing strongly interacted collinear microcracks. The level of σ^{∞} varies according to the different microcrack configurations generated by the computer. The statistical distribution of σ^{∞} gives rise to a failure probability vs normalized strength curve similar to the ones in Figs 3 and 4. The larger the number N_g, the more precise the numerical simulation for failure probability. Figure 5 shows the failure probability vs normalized strength curves by direct numerical simulations, contrasted to the similar curves furnished by the statistical approach. Figure 5(a), (b) correspond to case A and B, respectively. Calculations of the two cases are conducted under a crack density of $c_0/a_0 = 0.5$. The predictions from the two methods converge as the random generation number, N_g, becomes sufficiently large, as evidenced in Fig. 5. Good agreement between the two predictions justifies both approaches.

5. WEIBULL ANALYSIS

Weibull suggested the following three-parameter distribution for the strength data of brittle materials

$$W(\sigma) = 1 - \exp\left(-\left(\frac{\sigma - \sigma_u}{\sigma_0}\right)^m\right). \tag{34}$$

In eqn (34), $W(\sigma)$ is the cumulative failure probability at an applied stress σ that is normalized with respect to $K_{IC}/\sqrt{\pi a}$. The parameter σ_u denotes the location from which the cumulative failure probability starts to grow, and σ_0 characterizes the scale of the transition regime of a failure probability curve. The dimensionless parameter m is referred

to as the Weibull modulus which characterizes microcrack distribution in a brittle material. Equation (34) can be manipulated to a straight line of slope m on a lnln-ln Weibull plot

$$\ln\ln\left(\frac{1}{1-W(\sigma)}\right) = m\ln(\sigma-\sigma_u) - m\ln(\sigma_0). \tag{35}$$

If the cumulative failure probabilities obtained in the previous sections can be approximated by the Weibull distribution (34), then they should become straight lines in a Weibull plot. For both cases A and B, σ_u is equal to $\sigma_{th}^{\infty}\sqrt{\pi a_0}/K_{IC}$. The Weibull modulus can be determined by presenting the numerical data in a Weibull plot.

Figures 6 and 7 show the appropriateness of the three-parameter Weibull distribution function in fitting the strength data. As remarked by Sahimi and Arbabi (1993), the fitting by the three-parameter Weibull distribution relies on the randomness of the microstructure distribution in the material, the wider the distribution, the better the fitting. Such a trend is observed in Fig. 7(b), but not in Fig. 6(b). Nevertheless, in all cases plotted, the curves for different N become nearly straight lines parallel to each other. It seems that the Weibull modulus m is irrelevant to the number of microcracks. At the same time, the curves in Figs 6(a) and 7(a) reveal that the scale parameter σ_0 increases as N increases under fixed standard deviation. Typical $\ln(\sigma_0)$ vs s curves are plotted in Fig. 8 to illustrate the influence of the standard deviation s on the scale parameter σ_0. The curves show that $\ln(\sigma_0)$ decreases as s increases. Collecting data from these Weibull plots for different values of standard deviations, one can reveal the Weibull modulus vs standard deviation relation, as shown by the symbols in Fig. 9. Apparently, m decreases as s increases. The Weibull modulus m tends to zero as s becomes sufficiently large, and m tends to infinity near $s = 0$. Fitting those data points by the least-square method, one gets the following curve

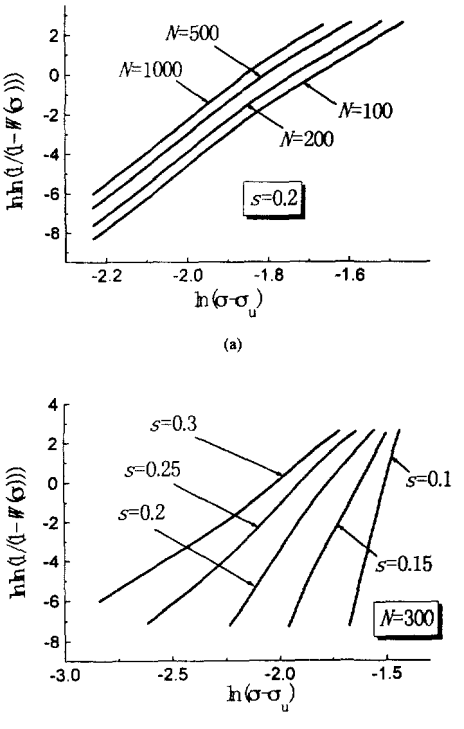

case A

Fig. 6. Weibull plots for case A: (a) $s = 0.2$; (b) $N = 300$.

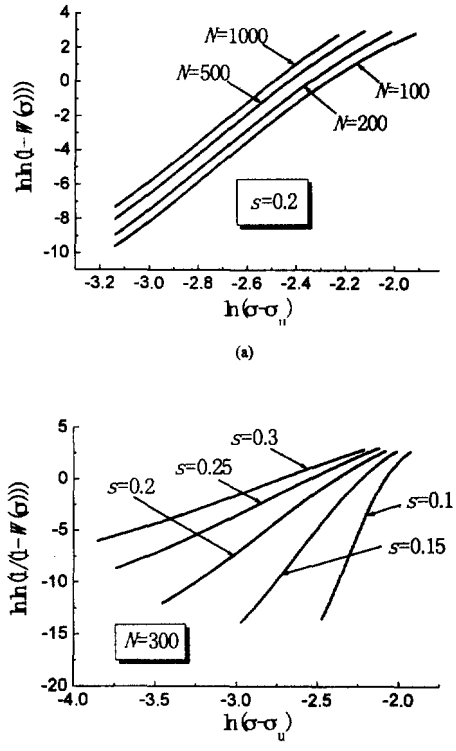

Fig. 7. Weibull plots for case B: (a) $s = 0.2$; (b) $N = 300$.

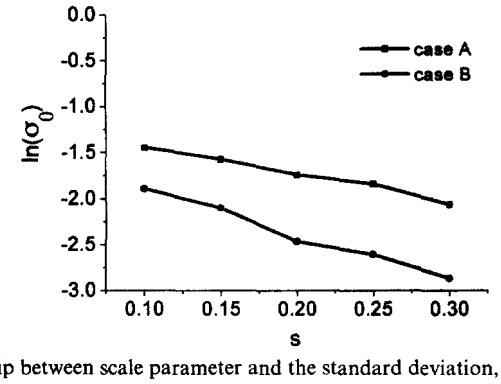

Fig. 8. Relationship between scale parameter and the standard deviation, case A and case B.

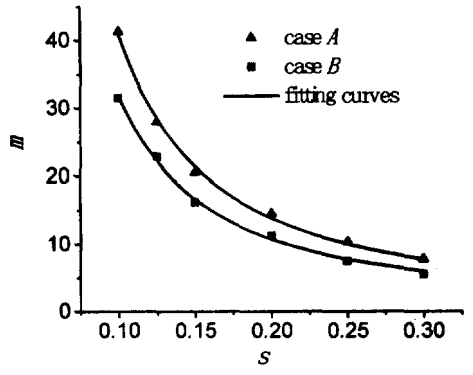

Fig. 9. Relationship between the Weibull modulus and the standard deviation, case A and case B.

$$m = \frac{d_1}{s} + \frac{d_2}{s^2} \tag{36}$$

where the fitting parameters are $d_1 = 1.44$, $d_2 = 0.26$ for case A, and $d_1 = 1.11$, $d_2 = 0.21$ for case B.

6. CONCLUDING REMARKS

The strength of a brittle solid containing microcracks depends not only on the average density of microcracks, but also on the fluctuation of microcracks, as manifested through the strong interaction between them. Furthermore, the scaling effect for the brittle solids can be quantified through the present model by considering the strong interaction between microcracks of fluctuated lengths and ligament sizes. These are the central messages of the present paper. For the simple case of collinear microcracks, the statistical model proposed here for failure prediction agrees reasonably well to the direct numerical simulation for configurations generated according to the given statistical characterization.

The statistical analysis also indicates that the strength distribution of brittle solids with collinear microcracks can be approximated by a three-parameter Weibull distribution. Moreover, the Weibull modulus appears independent of the size of the specimen. The size of the specimen mainly modifies the location of the strength transition, and scarcely perturbs transition characterization. Further investigations are required to certify if these conclusions hold true for the more general case of orientated planar microcracks.

Acknowledgements—The authors would like to thank the National Natural Science Foundation of China for the support of this research project. Joint supports by the Failure Mechanics Lab at Tsinghua University and the Solid Mechanics Lab at Tongji University are also acknowledged.

REFERENCES

Batdorf, S. B. and Crose, J. G. (1974) A statistical theory for the fracture of brittle structures subjected to non-uniform poly-axial stresses. *Journal of Applied Mechanics* **41,** 459–464.

Budiansky, B. and O'Connell, R. J. (1976) Elastic moduli of a cracked solid. *International Journal of Solids and Structures* **12,** 81–97.

Christensen, R. M. and Lo, K. H. (1979) Solutions for effective shear properties in three phase sphere and cylinder models. *Journal of Mechanics and Physics of Solids* **27,** 315–330.

Evans, A. G. (1978) A general approach for the statistical analysis of multiaxial fracture. *Journal of the American Ceramic Society* **61**(7–8), 302–308.

Evans, A. G. and Wiederhorn, S. M. (1984) Proof testing of ceramic materials—an analytical basis for failure prediction. *International Journal of Fracture* **26,** 355–368.

Gong, S. X. and Horii, H. (1989) General solution to the problem of microcracks near the tip of a main crack. *Journal of Mechanics and Physics of Solids* **37,** 27–46.

Kachanov, M. (1985) A simple technique of stress analysis in elastic solids with many cracks. *International Journal of Fracture* **28,** R11–19.

Kachanov, M. (1987) Elastic solids with many cracks: a simple method of analysis. *International Journal of Solids and Structures* **23,** 23–43.

Mori, T. and Tanaka, K. (1973) Average stress in matrix and average elastic energy of materials with misfitting inclusions. *Acta Metallurgica* **21,** 571–583.

Rice, J. R. (1968) Mathematical analysis in the mechanics of fracture. In *Fracture*, Vol. II, ed. H. Liebowitz, pp. 191–308. Academic Press, New York.

Rufin, A. C., Samos, D. R. and Bollard, R. J. H. (1984) Statistical failure prediction models for brittle materials. *AIAA Journal* **22,** 135–140.

Sahimi, M. and Arbabi, S. (1993) Mechanics of disordered solids: III fracture properties. *Physics Review B* **47,** 713–722.

She, S., Landes, J. D., Boulet, J. A. M. and Stoneking, J. E. (1991) Statistical theory for predicting the failure of brittle materials. *Journal of Applied Mechanics* **58,** 43–49.

She, S. and Landes, J. D. (1993) Statistical analysis of fracture in graphite. *International Journal of Solids and Structures* **63,** 189–200.

Tada, H., Paris, P. C. and Irwin, G. R. (1973) *The Stress Analysis of Cracks Handbook*. Del Research Corporation, Hellertown, Pennsylvania.

Taya, M. and Chou, T-W. (1981) On two kinds of ellipsoidal inhomogeneities in an infinite elastic body: an application to a hybrid composite. *International Journal of Solids and Structures* **17,** 553–563.

Weibull, W. (1939) A statistical theory of strength of materials. *Ingeniors Vetenskap Academiens*, Handlinger, no. 151.

Wiederhorn, S. M. and Fuller, E. R. Jr. (1985) Structural reliability of ceramic materials. *Material Science Engineering* **71,** 169–186.